LIMNOLOGY and OCEANOGRAPHY

ASLO

Limnol. Oceanogr. 66, 2021, 1687–1702

doi: 10.1002/lno.11713

A chemosynthetic ecotone—"chemotone"—in the sediments surrounding deep-sea methane seeps

Oliver S. Ashford [1]*, Shuzhe Guan [1], Dante Capone [1,2], Katherine Rigney [1,3], Katelynn Rowley [1], Victoria Orphan [4], Sean W. Mullin [4], Kat S. Dawson [5], Jorge Cortés [6], Greg W. Rouse [1], Guillermo F. Mendoza [1], Raymond W. Lee [7], Erik E. Cordes [8], Lisa A. Levin [1,9]

[1]Integrative Oceanography Division, Scripps Institution of Oceanography, University of California San Diego, La Jolla, California
[2]University of California Santa Cruz, Santa Cruz, California
[3]Carleton College, Northfield, Minnesota
[4]Division of Geological and Planetary Sciences, California Institute of Technology, Pasadena, California
[5]Department of Environmental Sciences, Rutgers, The State University of New Jersey, New Brunswick, New Jersey
[6]Centro de Investigación en Ciencias del Mar y Limnología, Universidad de Costa Rica, San José, Costa Rica
[7]Washington State University, Pullman, Washington
[8]Department of Biology, Temple University, Pennsylvania, 19122
[9]Center for Marine Biodiversity and Conservation, Scripps Institution of Oceanography, University of California San Diego, La Jolla, California

Abstract

Ecotones have been described as "biodiversity hotspots" from myriad environments, yet have not been studied extensively in the deep ocean. While physiologically challenging, deep-water methane seeps host highly productive communities fueled predominantly by chemosynthetic pathways. We hypothesized that the biological and geochemical influence of methane seeps extends into background habitats, resulting in the formation of a "chemotone" where chemosynthesis-based and photosynthesis-based communities overlap. To investigate this, we analyzed the macrofaunal assemblages and geochemical properties of sediments collected from "active," "transition" (potential chemotone), and "background" habitats surrounding five Costa Rican methane seeps (depth range 377–1908 m). Sediment geochemistry demonstrated a clear distinction between active and transition habitats, but not between transition and background habitats. In contrast, biological variables confirmed the presence of a chemotone, characterized by intermediate biomass, a distinct species composition (including habitat endemics and species from both active and background habitats), and enhanced variability in species composition among samples. However, chemotone assemblages were not distinct from active and/or background assemblages in terms of faunal density, biological trait composition, or diversity. Biomass and faunal stable isotope data suggest that chemotones are driven by a gradient in food delivery, receiving supplements from chemosynthetic production in addition to available photosynthetic-based resources. Sediment geochemistry suggests that chemosynthetic food supplements are delivered across the chemotone at least in part through the water column, as opposed to reflecting exclusively *in situ* chemosynthetic production in sediments. Management efforts should be cognisant of the ecological attributes and spatial extent of the chemotone that surrounds deep-sea chemosynthetic environments.

*Correspondence: oashford@ucsd.edu

Additional Supporting Information may be found in the online version of this article.

Author Contribution Statement: O.S.A. and L.A.L. conceived the study. E.E.C., V.O., L.A.L., J.C., and G.W.R. secured funding and facilitated collection of environmental data and biological samples. O.S.A., S.G., G.F.M., L.A.L., K. Rowley, and D.C. extracted biological specimens from samples. O.S.A., G.F.M., and G.W.R. identified the specimens. D.C., K. Rigney, and O.S.A. collected biomass data. O.S.A., S.G., D.C., K. Rigney, G.W.R., and L.A.L. contributed to the calculation of biodiversity and ecosystem functioning metrics. L.A.L. and O.S.A. prepared biological specimens for isotopic characterization, and R.W.L. undertook stable isotope measurements. S.W.M., K.S.D., and V.O. characterized sample geochemistry. O.S.A. undertook all other analyses and wrote the manuscript, which was contributed to, edited and revised by S.G., D.C., K. Rigney, K. Rowley, V.O., S.W.M., K.S.D., J.C., G.W.R., G.F.M., R.W.L., E.E.C., and L.A.L.

Ecotones and ecoclines

The related concepts of ecotones and ecoclines have their conceptual roots in the early 20th century (Livingston 1903; Clements 1905), and refer to zones of transition between organismal communities (Gosz 1993; Carney 2005; Kark and van Rensburg 2006). More specifically, an ecotone can be defined as a zone of transition among organismal communities, driven by a gradient of change in a key environmental variable, the characteristics of which vary strongly and abruptly over time (van der Maarel 1990; Attrill and Rundle 2002). An ecocline, in contrast, can be defined as a zone of transition between communities, driven by a gradient in a key environmental variable, the characteristics of which are relatively stable over time (van der Maarel 1990; Attrill and Rundle 2002).

Although ecotones and ecoclines, here jointly referred to as "transition zones," can occur across both time and space, we adopt a spatial perspective across ecological time frames, as opposed to geological time frames. In turn, transition zones can occur across a variety of spatial scales, such as between microhabitats, habitat patches, or between biomes (Gosz 1993), and the environmental variables that define them can be both abiotic and/or biotic in nature, and natural or anthropogenically influenced (Fortin et al. 2000).

Biological characteristics of transition zones

Transition zones have gained interest from ecologists and conservationists alike because of their particular biological characteristics. They have been described as "biodiversity hotspots," deserving of high conservation priority because they may host elevated species richness and faunal density, high levels of endemism and rarity, and be zones of enhanced hybridization and speciation rates relative to bordering communities. For example, in the first description of an ecotone between chemosynthetic and photosynthetic habitats, Meyer-Dombard et al. (2011) found ecotonal microbial assemblages to have a higher taxon diversity than surrounding assemblages. Walsh (1971) documented higher phytoplankton diversity in the ecotone of the Antarctic Convergence Zone relative to north and south of the convergence zone. Zajac et al. (2003) provide evidence for higher faunal densities in transition assemblages between shallow-water benthoscape elements, although species richness is not elevated in these transition zones relative to surrounding habitats. These combined features have been termed the "ecotone effect" (Odum 1953; Gosz 1993; Kark and van Rensburg 2006).

Transition zones in the deep sea

Because of the variety of circumstances that can produce transition zones, ecotones and ecoclines have been described from numerous environments and organismal communities (Kark and van Rensburg 2006). However, although likely to be widespread, transition zones in the deep ocean have not been extensively studied. Characterization of transition zones in the deep sea could help us to better understand, for example, the sensitivities of deep-sea species to environmental change, the prevalence of endemic species, and deep-sea speciation processes in general, thus improving our understanding of deep-ocean biodiversity as a whole. Some of the most conspicuous transition zones in the deep ocean occur between major depth divisions. Transitional assemblages may occur between shelf and bathyal, bathyal and abyssal, and abyssal and hadal bathymetric divisions (Carney 2005). This bathymetric zonation is thought to be determined by a suite of environmental variables that are correlated with water depth, including hydrostatic pressure, temperature, and food availability from photosynthetic sources (Carney 2005). For example, Flach and de Bruin (1999) found macrofaunal assemblages in the Northeast Atlantic Ocean to exhibit distinct shelf, slope, and abyssal faunal groups, and suggested these groups to be shaped by differences in organic matter supply as one moves downslope. Jamieson et al. (2011) provide evidence for an "ecotone" occurring between the depths of 6007 and 6890 m below sea level, between abyssal and hadal faunas. They attribute this ecotone (which perhaps may be more appropriately defined as an ecocline) to a change in depositional regime between abyssal and hadal environments.

Transition zones may also occur in the deep ocean between water masses with distinct oceanographic characteristics. For example, in the Faroe-Shetland Channel (Northeast Atlantic Ocean), cold, polar water meets with comparatively warm North Atlantic Water. At this boundary, centered at about 400 m water depth, the thermal gradient is large and variable over time, being influenced by mesoscale eddies. The boundary can be defined as an ecotone, hosting a mixture of "warm" and "cold" water fauna with an enhanced diversity, relative to surrounding water masses (Bett 2001; Gage 2004). The boundaries of oxygen minimum zones (OMZs) provide another example of transitional environments occurring between water masses with distinct oceanographic characteristics. Especially evident in benthic fauna when the OMZ boundary intersects the flanks of seamounts or continental slopes, these transition zones may exhibit enhanced faunal diversity relative to their bounding environments (Levin et al. 1991; Gooday et al. 2010).

Methane seeps and the "sphere of influence"

Deep-sea methane seeps are physiologically stressful environments, yet host highly productive communities that are fueled predominantly by chemical energy via chemosynthesis (Levin 2005; Demopoulos et al. 2010; Levin et al. 2016; Åström et al. 2018). They are patchily distributed along continental margins worldwide and are associated with the provision of a number of ecosystem services of global significance, including carbon sequestration through the production of authigenic carbonates, high rates of biogeochemical cycling, habitat provision to commercially important species, and

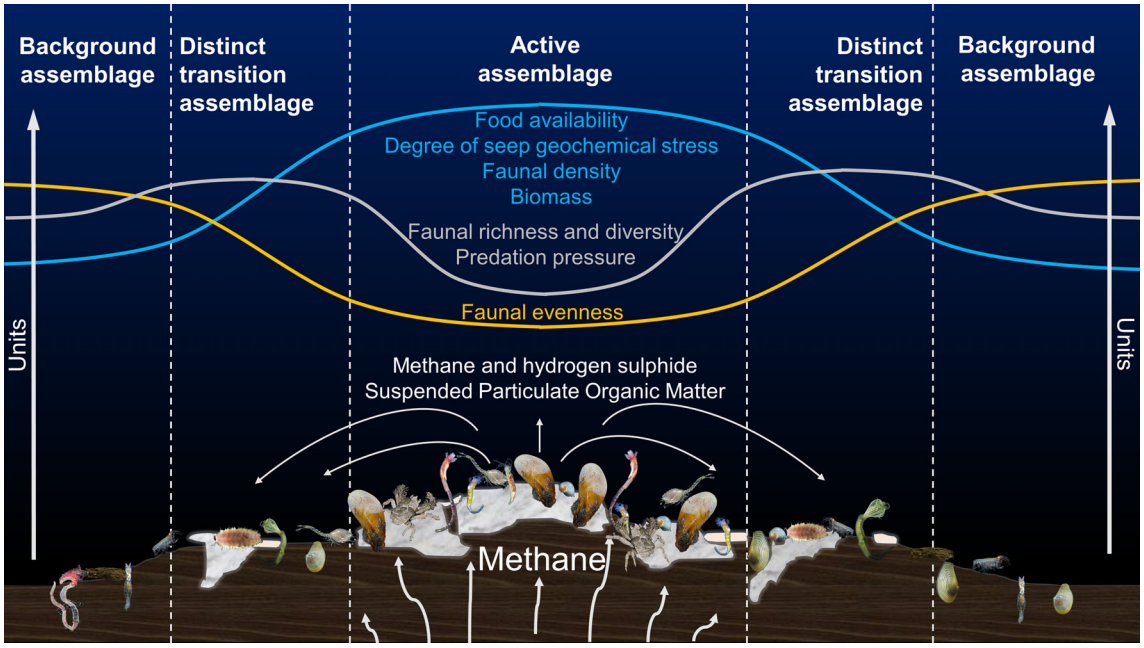

Fig 1. Conceptual diagram showing hypothesized characteristics of transition zone relative to surrounding active methane seep and background photosynthetically fueled deep-sea habitats.

bioprospecting potential (Boetius and Wenzhöfer 2013; Levin et al. 2016; Åström et al. 2020).

Levin et al. (2016) proposed that the biological and chemical influence of methane seeps extends out vertically and horizontally from the seep center into the overlying water column and down into underlying sediments to form a "sphere of influence" (Fig. 1). For example, methane, hydrogen sulfide, seep microbes, and particulate organic material may be advected away from the most active regions of seeps in near-bottom water, providing energy supplements to surrounding communities (McGinnis et al. 2006; Pohlman et al. 2011). Mobile predators may be attracted to productive seep communities (MacAvoy et al. 2002, 2003; Carney 2010; Åström et al. 2018), altering predation, disturbance, and nutrient regimes through their feeding and movement. The extent of influence of methane seeps on surrounding environments is likely to be variable over time, and so this transition zone between chemosynthetic seep environments and more typical photosynthetically based deep-sea environments may constitute an ecotone, or "chemotone."

Aims and hypotheses

Here, we analyze the biological (macroinfauna [> 300 μm] density, biomass, diversity, isotopic composition, species composition, and trait characteristics) and geochemical characteristics of sediments collected using push cores from and around methane seeps off the Pacific Coast of Costa Rica. We investigate whether a "chemotone" exists at the interface between chemosynthesis-based and photosynthesis-based ecosystems in the deep ocean, and examine whether methane seep transition zones exhibit unique characteristics compared to other ecotones linked with physiological stress and food gradients.

We hypothesized that transition zone sediments would exhibit a geochemical signature intermediate between active seep (high hydrogen sulfide concentration, high dissolved inorganic carbon [DIC] concentration, light $\delta^{13}C$ of DIC isotopic signature) and background sediments (low hydrogen sulfide concentration, low DIC concentration, heavy $\delta^{13}C$ of DIC isotopic signature). We hypothesized that macrofaunal assemblage characteristics would mirror sediment geochemistry patterns, and that the chemotone would exhibit a distinct taxonomic and trait composition relative to surrounding habitats, including the presence of habitat endemic species (species collected from only one of the three habitat types investigated) and an increased density of mobile, predatory taxa (Table 1; Fig. 1). We hypothesized that macrofaunal density and biomass in chemotone habitat would be greater than in background habitat, but lower than in active habitat, because of an intermediate degree of *in situ* chemosynthetic production and the delivery of food from active seep habitat (Table 1; Fig. 1), which would be illustrated by a faunal $\delta^{13}C$ isotopic signature intermediate in the chemotone between a lower signature of the chemosynthetic seep habitat and a higher signature of the photosynthetic background habitat. We further hypothesized that chemotone samples would have a significantly higher taxonomic and functional diversity than surrounding environments because of their incorporation of species from both chemosynthetic-based and photosynthetic-based communities (Table 1; Fig. 1).

Table 1. Hypotheses relating to the magnitude of biodiversity metrics and taxonomic and functional trait structure at methane seep transition zones, relative to active seeps and background sediments.

Hypothesis	Plausible mechanism for hypothesis	References supporting hypothesis
Transition samples exhibit a distinct taxonomic composition relative to active seep and background samples	Transition zone assemblages include species spilling over from bordering environments, and may contain habitat-endemic species, resulting in a distinct species composition. Low concentrations of methane and hydrogen sulfide in the water may facilitate specialized chemosynthetic symbioses	Odum (1953), Flach and de Bruin (1999), Jamieson et al. (2011), Meyer-Dombard et al. (2011), Goffredi et al. (2020)
Transition samples exhibit a distinct trait composition relative to active seep and background samples	Transition zone assemblages include an increased density of large, mobile, predatory macrofaunal taxa relative to background and active samples; attracted by higher food availability at seeps compared to background environments, but most unable to survive in the demanding chemical environment of active seeps	MacAvoy et al. (2002, 2003), Carney (2010)
Macrofaunal density, biomass, and $\delta^{13}C$ signature are intermediate in transition samples; higher/lighter than in background samples, but lower/heavier than in active seep samples	Subsidies from active seep habitat and *in situ* chemosynthetic production mean food availability at transition zones is intermediate between lower food availability at background sites, and greater food availability at active seep sites. Deep-sea assemblages are typically food-limited, so increasing food availability will increase faunal density and biomass	Rex et al. (2006), Johnson et al. (2007), Smith et al. (2008), Billett et al. (2010)
Macrofaunal richness and diversity are greatest in transition samples, relative to active seep and background samples	Transition zone assemblages include a mixture of species spilling over bordering environments, and may contain habitat-endemic species, causing elevated diversity in the transition zone	Odum (1953), Walsh (1971), Levin et al. (1991), Bett (2001), Kark and van Rensburg (2006), Gooday et al. (2010), Meyer-Dombard et al. (2011)
Macrofaunal evenness is intermediate in transition samples—lower than background samples, but higher than active seep samples	Food availability at seep transition zones is intermediate between lower food availability at background sites, and greater food availability at active seep sites. Assemblage evenness tends to decline with increasing food availability	Pearson and Rosenberg (1978), Weston (1990), Levin and Gage (1998), Cúrdia et al. (2004)

Methods

Sample collection

Sampling of sediments took place on the Costa Rican Pacific margin aboard RV *Atlantis* using the submersible *Alvin* over May–June 2017 (AT37-13) and October–November 2018 (AT42-03). Samples were collected from five methane seep sites (Jaco Scar, Mound 12, Mound 11, Parrita Seep, and Quepos Landslide) (Fig. 2; Supplementary Material 1: Fig. S1), covering a depth range of 377–1908 m. All samples were obtained under license of a collecting permit issued by the Ministerio de Ambiente y Energía of Costa Rica.

Multiple push cores (6.4 cm internal diameter) were taken at each sampling location. Of these, two were used for faunal characterization (data combined and treated as a single sampling point for statistical analyses—to avoid pseudoreplication; herein defined as a "sample"), and one of the remaining cores was used to characterize the geochemical environment (*see* Section 3.2). In total, 76 cores were used for faunal characterization, corresponding to 38 distinct sampling points (13 from Jaco Scar, 15 from Mound 12, 3 from Mound 11, 3 from Parrita Seep, and 4 from Quepos Landslide; *see* Supplementary Material 1: Fig. S1). At sea, the top 10 cm of sediment from each core was preserved in 8% formalin, and in the laboratory, samples were sieved through a 300 μm screen. Material retained was sorted for macrofauna at 12X magnification using a Wild M5A microscope. Annelid worms, peracarid crustaceans, and mollusks (95.7% of individuals collected; "macrofauna" herein) were identified to species or morphospecies level (2465 individuals, 204 species in total) (Dataset S2).

Sample habitat categorization

Samples were categorized as being collected from active, transition, or background habitats at the time of collection based on the relative proximity of visual indicators of seep activity. "Active" habitat was identified by large areas of microbial mats covering sediments, high seafloor cover of nonsedimented authigenic carbonates, and high densities of seep-associated megafauna, such as clams, mussels, siboglinid polychaetes, serpulid and sabellid polychaetes, frenulates, galatheid crabs, and the yeti crab, *Kiwa puravida* Thurber, Jones & Schnabel, 2011 (Mound 12 only). "Transition" habitat was identified by partially buried but visible authigenic

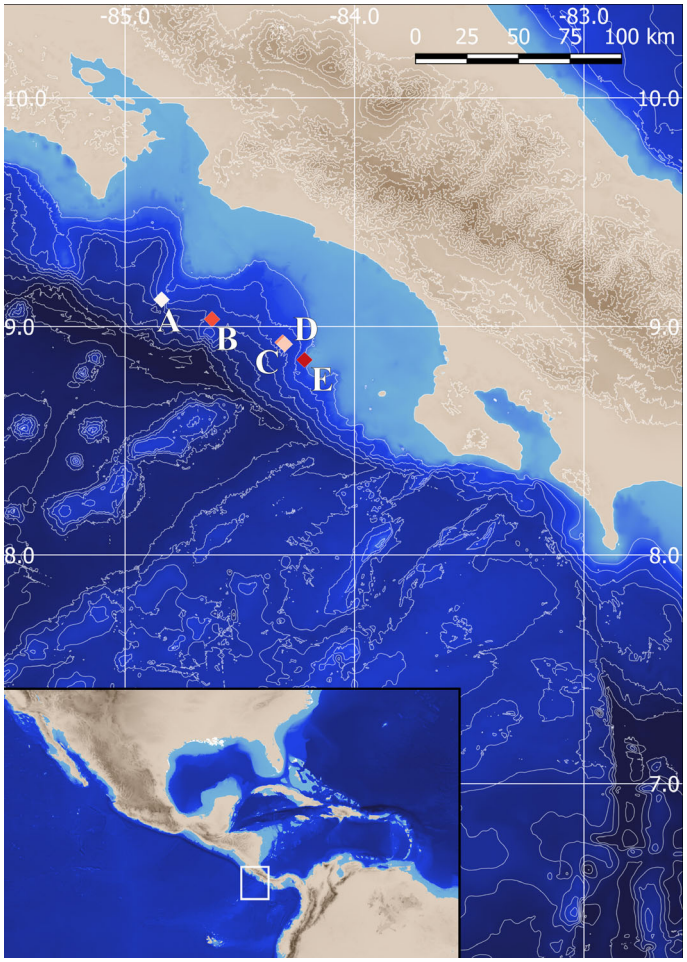

Fig 2. Sampling sites (white, and red-hue diamonds) in global and regional context. A: Jaco Scar; B: Parrita Seep; C: Mound 12; D: Mound 11; E: Quepos Landslide. Inset map places the sampled area (white box) in a global context. Bathymetry: darker blue areas = greater water depth, lighter blue areas = lesser water depth; 400 m depth contours; Global Multi-Resolution Topography (GMRT) 3.6 bathymetric data.

carbonates, scattered seep-associated megafauna, and shell remains of seep-associated bivalves. "Background" habitat was identified by the absence of authigenic carbonates, microbial mats, and seep-associated megafauna. In total, 13 faunal samples were collected from active habitat, 13 samples from transition habitat, and 12 samples from background habitat (Supplementary Material 1: Fig. S1). See Supplementary Material 1: Table S1 for details of average physical distances between samples within and among habitat categories for each seep site investigated.

Sediment geochemical characterization

Pore-water geochemistry was analyzed in 24 sediment cores paired with those used for faunal analyses. Geochemistry cores were extruded and sectioned into 1 cm horizons for the first 6 cm and 3 cm horizons for the remaining sediment. Each horizon was squeezed for pore water under Ar into a 30 mL disposable syringe using a Reeburgh-style squeezer (Reeburgh 1967) and immediately analyzed. Hydrogen sulfide concentrations were measured by an onshore Cline Assay after shipboard precipitation with zinc acetate (Cline 1969). Aliquots for DIC analysis were passed through 0.2 μm syringe filters into He-flushed 12 mL Exetainer vials with 100 μL 40% phosphoric acid. DIC concentration and carbon isotope composition ($\delta^{13}C$) were measured using a Gasbench II system interface to a Thermo Scientific Delta V Plus mass spectrometer (Thermo Scientific). Each sample was measured 10 times, and DIC peak areas and $\delta^{13}C$ DIC values (0.001 per mille instrument resolution) were average across those replicates. $\delta^{13}C$ DIC values were validated by comparison against standards of known isotopic composition across a range of concentrations. The geochemical characteristics of each sampling location were summarized as the maximal hydrogen sulfide and DIC concentrations, and minimal values of $\delta^{13}C$ DIC, recorded in the top 9 cm of cores analyzed for geochemistry.

Quantifying faunal density, biomass, and diversity

Faunal density was calculated as the total number of annelid, peracarid, and mollusk individuals per sample (two adjacent cores, each 32.17 cm^2 in surface area), multiplied by 155.42 (10,000 cm^2/ [32.17 $cm^2 \times 2$]) to express this as number of individuals per m^2, the standard unit for deep-sea faunal densities (Sanders et al. 1965). Faunal biomass (wet weight with shell) was measured to 0.01 mg using an electronic balance (A&D GR-202). Excess liquid was wicked from specimens using paper tissue, and final sample weights were recorded following a standardized 2-min period after removal from preservative. Biomass values per sample were multiplied by 155.42 to express them as g per m^2.

Biodiversity was quantified by both taxonomic and trait metrics. As taxonomic measures, species richness (number of species per sample), species diversity - Shannon Index (H′; natural logarithm), and species evenness - Pielou's Index (J′) were calculated in R 3.4.2 using the package "vegan" (Oksanen et al. 2013; R-CoreTeam 2017). To calculate metrics of trait diversity, a trait table was produced at the family level (lowest taxonomic level at which trait information was available for all taxa) following the methodology of Ashford et al. (2018) (Dataset S3). A list of traits scored and their relevance is given in Supplementary Material 1: Table S2. Continuous trait data ("maximum body length" and "maximum fecundity") were split into distinct categories based on natural breaks in the data (maximal values per family), identified using k-means clustering. Sturges' formula was used to determine an appropriate number of categories. This was undertaken in R 3.4.2 using the package "classInt" 0.1-22 (Bivand et al. 2015). To calculate metrics of trait diversity, for each sample, taxon-specific scores for each trait were weighted by taxon abundance and totaled across all taxa present. This produced a sample (rows) by trait abundance (columns)

matrix (Dataset S2), which was used to calculate trait richness, diversity, and evenness using the same methodology as for taxonomic diversity.

Macrofaunal isotopic characterization

Polychaete, peracarid crustacean, and molluscan individuals were opportunistically sampled for isotopic characterization ($\delta^{13}C$, $\delta^{15}N$) using 22 push cores and 3 sediment scoops collected from Jaco Scar, Mound 12, and Quepos Landslide during cruises AT37-13 and AT42-03 (Dataset S4). Sample habitat categories (active/transition/background) were assigned at the time of sampling based on the visual criteria listed above. At sea, specimens were washed in milli-Q water, placed in preweighed tin capsules using methanol-washed forceps, and stored at −20°C or −80°C. In the laboratory, tissue (0.2–1 mg dry weight) was acidified in 2 N H_3PO_4 to remove inorganic carbon. Stable isotope measurements were made using a Costech elemental analyzer and Micromass Isoprime isotope ratio mass spectrometer (EA/IRMS). Stable isotope ratios ($\delta^{13}C$, $\delta^{15}N$) are expressed in the standard δ (delta) notation, using the Pee Dee Belemite standard for $\delta^{13}C$, and atmospheric nitrogen for $\delta^{15}N$ (Fry 2006). Precision for $\delta^{13}C$ and $\delta^{15}N$ analyses were ± 0.02‰ and ± 0.05‰ respectively (standard deviation of 10 replicate organic standards). In total, 50 individuals from active habitat, 31 individuals from transition habitat, and 7 individuals from background habitat were characterized for stable isotope composition.

Statistical analyses

Prior to analysis, sample "AD4919, PC4 + PC8" (Quepos Landslide, Active) was removed from the dataset because it contained no macrofauna. Differences in the values of faunal density and biomass, univariate biodiversity metrics, and geochemical variables amongst activity habitats were investigated under a generalized linear model (GLM) framework using R v3.4.2 (R-CoreTeam 2017). Seep site and sampling cruise were included as covariates to statistically control for differences amongst sites and between sampling cruises. A GLM framework was selected to facilitate flexibility in the choice of error distribution and link function. Appropriate error distributions and link functions for each model were selected based on data characteristics (e.g., count vs. continuous data), model diagnostics, and the Akaike information criterion (AIC) (Supplementary Material 1: Table S5). Where count data were modeled, overdispersion was checked for by calculation of the dispersion parameter "theta" (theta = residual deviance / residual degrees of freedom) and corrected for as appropriate. Models were simplified by backward stepwise selection based on independent variable *p*-values until a minimum model AIC value was achieved. Rarefaction species richness curves were plotted for each activity habitat using the R package "vegan" (Oksanen et al. 2013).

Dissimilarity in species and trait composition among habitats and seep sites was evaluated in PRIMER v6 (Clarke and Gorley 2006) using two-way crossed analysis of similarities (ANOSIM), based on the Bray–Curtis dissimilarity metric (9999 permutations). Two-way crossed similarity percentage (SIMPER) analysis was performed in PRIMER v6 (Clarke and Gorley 2006) to identify the percent contribution of species and traits to the Bray–Curtis dissimilarity within and between activity habitats and seep sites (9999 permutations). To investigate potential differences amongst seep sites, one-way ANOSIM and SIMPER analyses were additionally conducted for Mound 12 and Jaco Scar seep sites (the two best-sampled sites in this investigation, as well as in past biological investigations of Costa Rica's methane seeps). Nonmetric multidimensional scaling (nMDS) analysis, based on the Bray–Curtis dissimilarity metric, was performed using the R package "vegan" (Oksanen et al. 2013) to visualize the species and trait dissimilarity of samples.

An alpha value of 0.05 was applied to all statistical tests.

Results

Geochemical variables

As hypothesized, sediment geochemistry in transition habitat was distinct from that in active habitat (Fig. 3; Table 2). Maximal hydrogen sulfide and DIC concentrations were significantly lower in samples from transition habitat than in samples from active habitats ($t(16) = 5.816$, $p < 0.001$; $t(12) = 4.211$, $p = 0.001$, respectively), and minimum carbon isotope ($\delta^{13}C$) values of DIC in samples from transition habitat were significantly heavier than in samples from active habitat ($t(15) = -9.121$, $p < 0.001$) (Fig. 3). However, contrary to our hypothesis, sediment geochemistry in transition habitat was not distinct from that of background habitat (Table 2; Fig. 3). Maximal hydrogen sulfide and DIC concentrations, and minimum carbon isotope ($\delta^{13}C$) values of DIC were not significantly different between samples from transition and background habitats ($t(16) = 0.217$, $p = 0.831$; $t(12) = -1.624$, $p = 0.130$; $t(15) = 0.022$, $p = 0.983$, respectively) (Fig. 3). There was no significant influence of seep site on the values of any of the geochemical variables measured.

Macrofaunal density, biomass, and isotopic signatures

As hypothesized, macrofaunal density was greater in samples collected from active habitat than in samples collected from transition habitat ($z(33) = 5.491$, $p < 0.001$) (Table 2; Fig. 3D). However, contrary to our hypothesis, macrofaunal density in transition habitat was not significantly distinct from that in background habitat ($z(33) = -0.415$, $p = 0.678$) (Table 2; Fig. 3D). Unlike density, and consistent with our hypothesis, macrofaunal biomass in transition samples was intermediate between the higher biomass of samples from active habitat ($t(30) = 4.103$, $p < 0.001$), and the lower biomass of samples from background habitat ($t(30) = -3.415$, $p = 0.002$) (Table 2; Fig. 3E). As hypothesized, the average $\delta^{13}C$ value of macrofaunal individuals collected from transition

habitat (−28.66; SE = ±1.09‰) was intermediate between those collected from active (−33.38; SE = ±1.19‰) and background (−21.73; SE = ±0.98‰) habitats (Table 2). The average $\delta^{15}N$ value of individuals collected from transition habitat (5.71; SE = ±0.94‰) was similar to that collected from active (5.25; SE = ±0.53‰) or background (5.20; SE = ±1.32‰) habitats (Table 2).

Macrofaunal diversity

Contrary to our hypothesis, species richness in transition samples was not significantly greater than in samples collected from active or background habitats ($t(30) = -0.897$, $p = 0.377$; $t(30) = 0.528$, $p = 0.601$, respectively) (Table 2; Fig. 3F). Furthermore, while species diversity (Shannon Index) and evenness (Pielou's Index) in transition samples were significantly greater than in samples collected from active habitat ($t(29) = 3.510$, $p = 0.001$; $t(30) = 2.108$, $p = 0.044$, respectively), they were not significantly different from samples collected from background habitat ($t(29) = -0.405$, $p = 0.689$; $t(30) = -0.979$, $p = 0.335$, respectively) (Table 2; Fig. 3G,H). Consistent with these observations, rarefaction demonstrated active habitat to host a lower diversity of macrofaunal species than transition and background habitat, which host a similar diversity of macrofaunal species (Fig. 4).

In contrast to our hypotheses, we found no influence of seep habitat on trait diversity metrics. Transition samples did not have a significantly distinct functional trait richness, diversity or evenness compared to samples collected from active habitat ($z(30) = 0.027$, $p = 0.979$; $t(30) = 1.010$, $p = 0.321$; $t(30) = 1.058$, $p = 0.298$, respectively), or background habitat ($z(30) = 0.052$, $p = 0.958$; $t(30) = 1.198$, $p = 0.240$; $t(30) = 1.219$, $p = 0.232$, respectively) (Table 2).

Species composition

As hypothesized, species composition differed among the activity habitats (ANOSIM, Global R = 0.667, $p < 0.001$). Samples collected from transition habitat had a distinct species composition compared to samples collected from active (ANOSIM, R = 0.751, $p < 0.001$) and background (ANOSIM, R = 0.272, $p = 0.003$) habitats (Fig. 5A,B). Transition and active samples had an average Bray–Curtis dissimilarity of 94.5%. SIMPER analysis suggests that half of this dissimilarity was driven by lower abundances in samples taken from transition habitat, relative to active habitat, of the cumacean family Leuconidae, the polychaetes families Ampharetidae, Dorvilleidae, Hesionidae, and Siboglinidae, and the gastropod family Skeneidae (in order of decreasing influence). Transition and background samples had an average Bray–Curtis dissimilarity of 76.4%, where 50% of this dissimilarity was driven by higher abundances in samples taken from transition habitat, relative to background, of the polychaete families Maldanidae, Paraonidae, Flabelligeridae, Siboglinidae, Cirratulidae and Cossuridae, the tanaidacean families Pseudotanaidae, Tanaellidae, and Anarthruridae, and the mollusk families Skeneidae, Cuspidaridae, and Vesicomyidae, and lower abundances of the polychaete families Spionidae, Chrysopetalidae, Dorvilleidae, Capitellidae, and Hesionidae, aplacophoran mollusks, the bivalve family Nuculanidae, and the tanaidacean family Agathotanaidae (in order of decreasing influence). Samples collected from transition habitat were more variable in their species composition (average assemblage similarity of 19.8%), than samples collected from active (average assemblage similarity of 37.0%) or background habitats (average assemblage similarity of 34.8%).

Only 30 species (15% of the 204 species present in this study) were collected exclusively from transition habitat (putative transition habitat endemics). These included species in the peracarid families Ischyroceridae, Munnopsidae, and Leptognathiidae, and selected species of the polychaete families Amphinomidae, Glyceridae, Phyllodocidae, Sabellidae, and Spionidae, and the bivalve family Nuculanidae. In comparison, 25 species were collected exclusively from active habitat (putative active habitat endemics, particularly species of the polychaete families Amphinomidae, Dorvilleidae, Hesionidae, the mollusk family Hyalogyrinidae, and the amphipod family Oedicerotidae, and also select species of the polychaete families Cirratulidae, Polynoidae, and Spionidae, and the mollusk family Nuculanidae), and 44 species were collected exclusively from background habitat (putative background habitat endemics, particularly species of the polychaete families Opheliidae and Oenonidae, and the peracarid families Agathotanaidae, Desmosomatidae, Diastylidae, Pardaliscidae, and Typhlotanaidae) (Table 3).

Forty species were found to occur across all three activity habitats (habitat "generalists"; particularly selected species of the polychaete families Cirratulidae, Cossuridae, and Paraonidae, and the bivalve families Cuspidaridae and Nuculanidae). Sixteen species were collected from both transition and active habitat, but not from background habitat (particularly selected species of the polychaete families Hesionidae, Maldanidae, and Sabellidae, the mollusk families Vesicomyidae and Skeneidae, and the tanaid family Anarthruridae, suggesting spillage of species from active habitat into transition habitat); 36 species were collected from both transition and background habitat, but not active habitat (particularly selected species of the polychaete families Ampharetidae, Capitellidae, Cirratulidae, Flabelligeridae, Paralacydonidae, and Sabellidae, suggesting spillage of species from background habitat into transition habitat). Twelve species were collected from both active and background habitat, but not transition habitat (Table 3; Supplementary Material 1: Table S3), possibly reflecting undersampling of these mostly rare taxa.

Singletons (one specimen of a species) were common in all the habitats studied.

In transition habitat, of the 122 species identified, 52 (42.6%) were represented by only one individual, compared to 34 singletons (36.6%) of the 93 species identified for

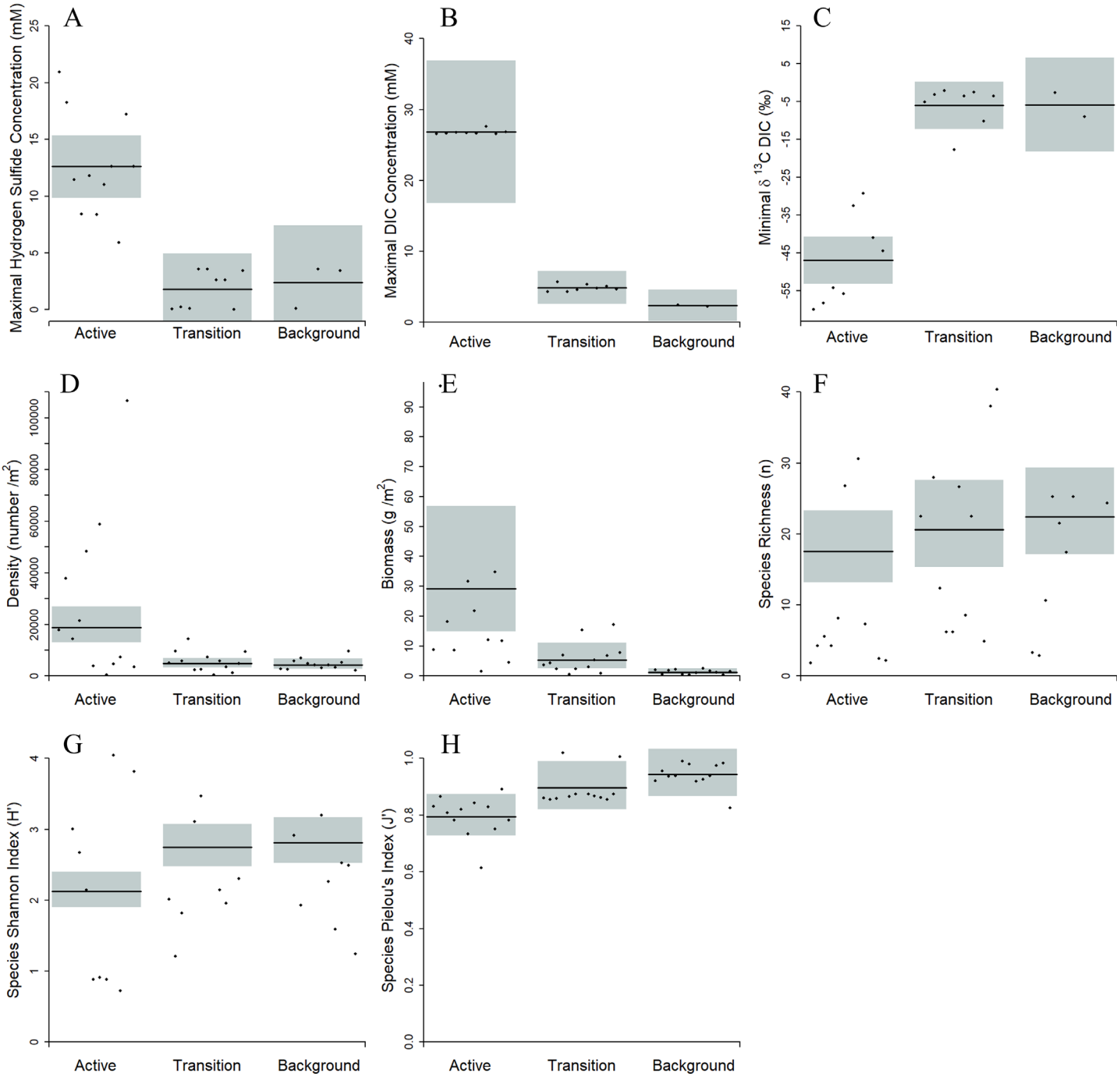

Fig 3. Values of geochemical and biological variables at active, transition and background habitats; (**A**) maximal hydrogen sulfide (HS^- and H_2S) concentration, (**B**) maximal dissolved inorganic carbon (DIC) concentration, (**C**) minimal $\delta^{13}C$ value of DIC, (**D**) macrofaunal density, (**E**) macrofaunal biomass, (**F**) species richness, (**G**) species diversity – Shannon Index (H′), (**H**) species evenness – Pielou's Index (J′). Partial plots, bars are mean values, gray envelopes are 95% confidence intervals, points are partial residuals not raw data.

active habitat, and 60 singletons (45.5%) of the 132 species identified for background habitat. Please see Supplementary Material 1: Table S3 for full SIMPER results.

Assemblage analyses undertaken individually for Mound 12 and Jaco Scar seeps were congruent with the two-way analyses undertaken on all seep sites combined (ANOSIM, Global R = 0.852, $p < 0.001$; ANOSIM, Global R = 0.406, $p = 0.002$, respectively). Mound 12 samples collected from transition habitat had a significantly distinct species composition compared to samples collected from active (ANOSIM, R = 1.000, $p = 0.005$) and background (ANOSIM, R = 0.306, $p = 0.016$) habitat. Jaco Scar samples collected from transition habitat

Table 2. Mean ± standard error (in brackets) per habitat for macrofaunal density and biomass, biodiversity metrics, and geochemical metrics. N = number of samples for all metrics except "Infauna $\delta^{13}C$ (‰)" and "Infauna $\delta^{15}N$ (‰)," where N = number of individuals. Note: sample "AD4919, PC4 + PC8" (Quepos Landslide, Active) with zero macrofauna is included here, but not in statistical analyses.

Habitat	Density (n/m^2)	Biomass (g/m^2)	Species richness (n)	Trait richness (n)	Species diversity (Shannon Index H')	Trait diversity (Shannon Index H')	Species evenness (Pielou's Index J')	Trait evenness (Pielou's Index J')	Maximal [hydrogen sulfide] (mM)	Maximal [dissolved inorganic carbon] (mM)	Minimum $\delta^{13}C$ of DIC (‰)	Infauna $\delta^{13}C$ (‰)	Infauna $\delta^{15}N$ (‰)
Transition	5356(±699) N=13	20.49(±12.05) N=13	18.23(±2.26) N=13	29.31(±0.87) N=13	2.41(±0.26) N=13	2.93(±0.04) N=13	0.86(±0.05) N=13	0.87(±0.01) N=13	0.09(±0.02) N=9	5.03(±1.24) N=8	−4.68(±1.65) N=8	−28.66(±1.09) N=31	5.71(±0.94) N=31
Active	19,081(±4896) N=13	79.43(±43.50) N=13	15.23(±3.38) N=13	27.54(±2.36) N=13	1.89(±0.22) N=13	2.75(±0.23) N=13	0.73(±0.07) N=13	0.81(±0.07) N=13	9.96(±1.87) N=12	22.37(±4.18) N=9	−44.16(±4.31) N=9	−33.38(±1.19) N=50	5.25(±0.53) N=50
Background	5453(±498) N=12	2.71(±0.57) N=12	22.75(±1.78) N=12	30.50(±0.47) N=12	2.94(±0.08) N=12	3.00(±0.03) N=12	0.95(±0.01) N=12	0.88(±0.01) N=12	0.07(±0.04) N=3	3.32(±0.91) N=2	−3.25(±1.38) N=2	−21.73(±0.98) N=7	5.20(±1.32) N=7

had a near/marginally statistically distinct species composition compared to samples collected from active (ANOSIM, R = 0.323, p = 0.054) and background (ANOSIM, R = 0.244, p = 0.048) habitat.

Trait composition

Trait composition differed amongst the activity habitats (ANOSIM, Global R = 0.459, $p < 0.001$) (Fig. 5C,D). Samples collected from transition habitat had a significantly distinct trait composition relative to active habitat (ANOSIM, R = 0.693, $p < 0.001$), but, contrary to our hypothesis, did not have a distinct trait composition relative to background habitat (ANOSIM, R = 0.074, p = 0.176). Transition and active habitat samples had an average Bray–Curtis dissimilarity of 59.4%. SIMPER analysis suggests that half of this dissimilarity was driven by lower expression in transition habitat, relative to active, of the traits of small maximum adult body size, tube or burrow dweller, infaunal habitat space, lecithotrophic reproductive strategy, low maximal fecundity, deposit feeding, and epibenthic habitat space (in order of decreasing influence). The same set of traits also drives dissimilarity between background and active habitats. Samples collected from transition habitat were more variable in their trait composition (average assemblage similarity of 71.2%), than samples collected from background habitat (average assemblage similarity of 81.6%), but were less variable in their trait composition than samples collected from active habitat (average assemblage similarity of 63.5%). Of the 15 most frequently expressed traits in each activity habitat, 86.7% were shared between transition and active habitats, 100% were shared between transition and background habitats, and 86.7% were shared between background and active habitats. All analyzed traits were found to be expressed to some extent in all activity habitats. Please see Supplementary Material 1: Table S4 for full SIMPER results.

Results of analyses undertaken individually for Mound 12 and Jaco Scar seeps were congruent with the two-way analyses undertaken on all seep sites combined (ANOSIM, Global R = 0.589, $p < 0.001$; ANOSIM, Global R = 0.284, p = 0.021, respectively). Mound 12 samples collected from transition habitat had a significantly distinct trait composition relative to active habitat (ANOSIM, R = 0.893, p = 0.005), but did not have a distinct trait composition relative to background habitat (ANOSIM, R = −0.031, p = 0.54). Jaco Scar samples collected from transition habitat had a near-significantly distinct trait composition relative to active habitat (ANOSIM, R = 0.405, p = 0.054), but did not have a distinct trait composition relative to background habitat (ANOSIM, R = 0.152, p = 0.111).

Discussion

Evidence for a chemotone

Our results provide evidence for a subtle, yet distinct "chemotone" in the sediments surrounding deep-sea methane seeps that does not appear to be driven by sediment

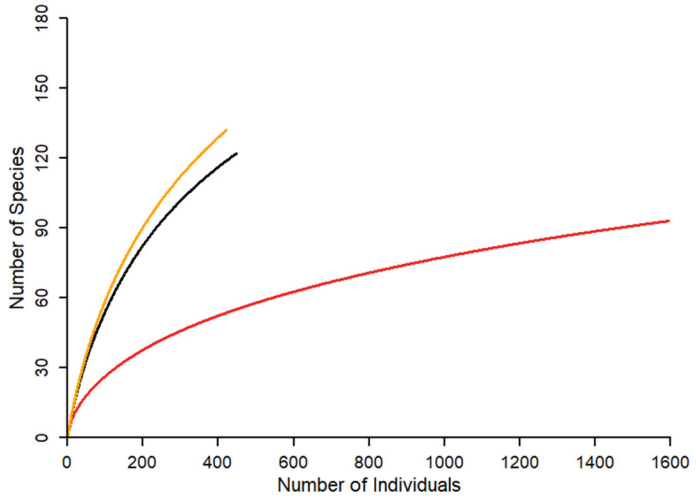

Fig 4. Rarefaction curves showing expected number of species as a function of number of individuals collected from active (red), transition (orange) and background (black) habitats.

geochemistry. This chemotone is characterized by intermediate macrofaunal biomass (1/4 that of active habitat, but ~ 8X greater than background habitat; Fig. 3E), a distinct species composition (Fig. 5A,B), including species from both active and background habitats (such as species of the polychaete families Ampharetidae, Cirratulidae, Flabelligeridae, Glyceridae, Maldanidae, Paralacydonidae, Phyllodocidae, Sabellidae, Spionidae, the mollusk families Nuculanidae and Vesicomyidae, and tanaidaceans), as well as numerous habitat endemic species (particularly peracarid crustacean and sabellid polychaete species), and a greater variability in species composition between samples than in active or background habitats.

While chemotone samples exhibited distinct geochemical signatures, trait composition, higher species diversity and evenness, higher proportion of singletons, and lower faunal density relative to active habitats, they were not distinct from background samples in these characteristics (Figs. 3–5). Thus, in terms of α diversity metrics, faunal density, and rarity, we did not find evidence for a strong "ecotone effect" (Odum 1953; Gosz 1993; Kark and van Rensburg 2006). It is possible that this finding reflects relatively low statistical power in our dataset (38 samples in total), and collection of additional samples would help to determine whether these results are true patterns or type II errors. We did, however, identify a number of species recorded only from the chemotone habitat (putative chemotone endemics, particularly species of peracarid crustacean and sabellid polychaete), giving the possibility that chemotones are zones of speciation.

Comparison of results with previous studies at deep-sea chemosynthetic environments and other zones of environmental stress

Studies of methane seep fauna to date have typically compared active seep habitat with background habitat, such as Levin and Mendoza (2007), Menot et al. (2010), Leduc et al. (2016), Campanyà-Llovet and Snelgrove (2018), and Sen et al. (2019) (*see* Levin et al. (2016) for a review), and, to the best of our knowledge, this study is the first to investigate the characteristics of the transition zone macrofauna relative to active seep and background habitats. However, some studies of deep-sea hydrothermal vent communities have investigated whether a distinct transition fauna surrounds hydrothermal vents. For example, studies investigating the composition of megafaunal assemblages surrounding hydrothermal vents provide evidence for a "peripheral fauna" between active vent and background deep-sea habitats (Hessler and Smithey 1983; Marcus and Tunnicliffe 2002; Gerdes et al. 2019; Alfaro-Lucas et al. 2020; Georgieva et al. 2020). Similar to our results, vent transition zones do not typically display sediment temperature or sulfide anomalies, and are characterized by a mixture of both vent and background deep-sea species, and higher faunal evenness, but a similar taxonomic richness, relative to active vent habitat (Marcus and Tunnicliffe 2002; Sen et al. 2016).

Considering α diversity metrics, our finding that chemotone samples were no richer, more even, or more diverse than background habitat samples contrasts with those of studies investigating ecotones associated with gradients of environmental stress. For example, transition zones at the boundary of OMZs may exhibit enhanced faunal diversity relative to their bounding environments (Levin et al. 1991; Gooday et al. 2010). Transition zones attributable to temperature stress, such as occur in the Faroe-Shetland Channel, may be characterized by enhanced diversity compared to surrounding water masses (Bett 2001; Gage 2004). Microbial assemblages in an ecotone between freshwater chemosynthetic and photosynthetic environments have been demonstrated to exhibit enhanced taxon diversity (Meyer-Dombard et al. 2011), and transition habitats along gradients of salinity may have higher (Traut 2005) or lower species diversity (Nebra et al. 2016).

However, our finding of a distinct chemotone species composition is in agreement with studies of ecotones across zones of environmental stress. For example, ecotones along stress gradients of salinity and temperature have been shown to exhibit distinct assemblage compositions relative to surrounding habitats, characterized by a mix of species from surrounding communities (Bett 2001; Attrill and Rundle 2002; Gage 2004; Traut 2005). These results are consistent with the suggestion that ecotones are most clearly identified by investigations of patterns of β diversity, as opposed to α diversity (Koulouri et al. 2006).

Environmental drivers of chemotones and the "sphere of influence"

We predicted that any chemotone identified between active seep and background habitats would be driven, in part, by gradients in seep sediment geochemistry, such as hydrogen sulfide concentration. However, while the particulars of sediment geochemistry may be chiefly responsible for driving the observed distinction between active habitat, and transition

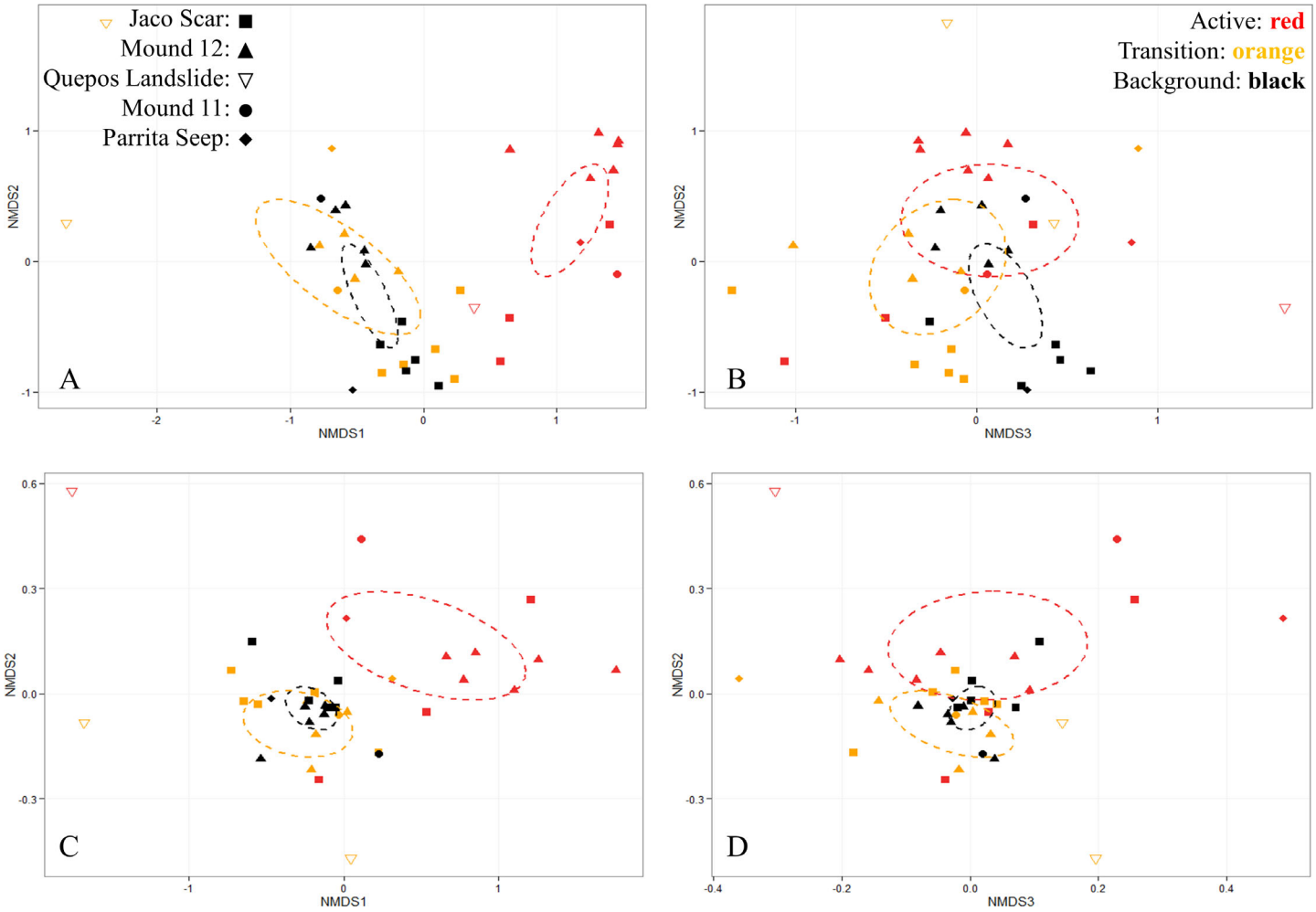

Fig 5. Nonmetric multidimensional scaling (nMDS) plots (Bray–Curtis dissimilarity) of samples based on species (stress: 0.094) and trait data (stress: 0.020) weighted by abundance. Color reflects habitat; active: red; transition: orange; background: black. Point shape reflects seep site; Jaco Scar: square; Mound 12: triangle; Quepos Landslide: upside-down triangle; Mound 11: circle; Parrita Seep: diamond. (**A**) Species data, axes 1 and 2, showing distinction in species composition between active, and transition and background samples. (**B**) Species data, axes 2 and 3, showing distinction in species composition between transition and background samples. (**C**) Trait data, axes 1 and 2, showing distinction in trait composition between active, and transition and background samples. (**D**) Trait data, axes 2 and 3, showing no distinction in trait composition between transition and background samples. 95% confidence ellipses displayed.

and background habitats (Figs. 3–5) (Levin 2005), the geochemical characteristics of chemotone and background habitats were not statistically distinguishable (Fig. 3). This suggests a highly localized influence of subsurface seepage on the macroinfauna, and that observed faunal distinctions between chemotone and background assemblages are not driven by the measured seep sediment geochemistry parameters. This is in agreement with studies of peripheral assemblages surrounding hydrothermal vents (Marcus and Tunnicliffe 2002; Sen et al. 2016). Instead, our finding of significantly elevated macrofaunal biomass in the chemotone, relative to background habitat (Fig. 3E), suggests that assemblage differences between these habitats could be driven by differences in food availability. Chemotones may benefit from energy supplements from active chemosynthetic habitats transported via the water column, including methane and/or hydrogen sulfide that fuel seep microbes themselves, and particulate organic material (McGinnis et al. 2006; Pohlman et al. 2011; Alfaro-Lucas et al. 2020; Georgieva et al. 2020).

We speculate that suspension and filter feeding taxa in the chemotone may utilize these energy supplements directly from the water column, while deposit feeding taxa may benefit from increased food availability in the chemotone sediments. For instance, some taxa among our chemotone habitat endemics, such as suspension feeding serpulid and sabellid polychaetes, have recently been demonstrated to utilize methane at low concentrations in near-bottom water as an energy source for methane oxidizing microbial symbionts farmed on their tentacular crown (Goffredi et al. 2020). This supports the suggestion that seeps deliver food supplements directly to

Table 3. Ten most abundant species in each habitat type (in order of abundance) for all seep sites combined, and for Mound 12 and Jaco Scar in isolation. Percent contribution of each species to total abundance within habitat and site combination given. Letter codes reflect level of habitat specialization for species within site category: A = collected from active habitat; T = collected from transition habitat; B = collected from background habitat; no letters = collected from all three habitat categories.

Habitat	All seep sites Species	% total abund.	Mound 12 Species	% total abund.	Jaco Scar Species	% total abund.
Transition	*Tanaella c.f. rotundicephala* T+B	8.48	*Parougia* sp. 1	6.08	Maldanidae sp. 1	13.42
	Amphisamytha sp. 1 T+B	8.26	Nuculanidae sp. 4	5.41	*Pseudotanais c.f. corollatus*	7.38
	Maldanidae sp. 1	5.13	Siboglinidae sp. 1 T+A	5.41	Spionidae sp. 5	6.04
	Spionidae sp. 5	4.46	*Spiophanes* sp. 1	5.41	Nuculanidae sp. 4	4.03
	Spiophanes sp. 1	4.02	Paraonidae sp. 2	4.73	*Fucaria* sp. 1 T+A	4.03
	Nuculanidae sp. 4	3.13	Ampharetidae sp. 3 T+B	4.05	Cossuridae sp. 3	4.03
	Paraonidae sp. 2	2.68	Spionidae sp. 5 T+B	4.05	Maldanidae sp. 6 T+A	2.68
	Pseudotanais c.f. corollatus	2.68	*Brada* sp. 1 T+B	3.38	*Cuspidaria* sp. 1	2.68
	Parougia sp. 1	2.46	*Cossura* sp. 1	2.70	*Brada* sp. 1 T	2.01
	Brada sp. 1 T+B	2.00	Cirratulidae sp. 2 T+B	2.70	Paraonidae sp. 2 T+B	2.01
Active	*Paraleucon* nov.sp. A+B	18.55	*Paraleucon* nov sp. A+B	25.15	Hesionidae sp. 3 A	22.05
	Ampharetidae sp. 1 T+A	15.41	Ampharetidae sp. 1 A	20.70	*Fucaria* sp. 1 T+A	7.25
	Fucaria sp. 1 T+A	14.10	*Fucaria* sp. 1 A	15.83	Nuculanidae sp. 4	6.65
	Hesionidae sp. 3 A	8.65	Dorvilleidae sp. 2 A	9.07	Cossuridae sp. 3	6.35
	Dorvilleidae sp. 2	7.71	Hesionidae sp. 2 T+A	4.96	Cossuridae sp. 2 A+B	5.74
	Hesionidae sp. 2 T+A	4.82	Ampharetidae sp. 2	3.34	Cirratulidae sp. 9 A	4.83
	Ampharetidae sp. 2	3.20	Hesionidae sp. 3 A	3.08	Hesionidae sp. 2 A	4.53
	Ophryotrocha sp. 3 A+B	2.82	*Ophryotrocha* sp. 3 A+B	2.91	Dorvilleidae sp. 2	4.23
	Siboglinidae sp. 1	2.19	Siboglinidae sp. 1 T+A	2.65	Nuculanidae sp. 2 A	3.32
	Nuculanidae sp. 4	1.50	Capitellidae sp. 2	1.28	*Hesione* sp. 3 A	3.02
Background	Spionidae sp. 5	7.13	*Spiophanes* sp. 1	11.18	Spionidae sp. 5	12.57
	Spiophanes sp. 1	6.65	*Parougia* sp. 1	6.83	Nuculanidae sp. 4	8.57
	Nuculanidae sp. 4	5.23	Ampharetidae sp. 3 T+B	4.35	*Micospina aureobohnorum* T+B	5.71
	Micospina aureobohnorum	3.33	Cirratulidae sp. 4	4.35	Aplacophora sp. 6 A+B	2.86
	Parougia sp. 1	3.33	Nuculanidae sp. 4	4.35	Cirratulidae sp. 6 B	2.29
	Ampharetidae sp. 3 T+B	2.61	Paraonidae sp. 2	4.35	*Macrochaeta* sp. 1 T+B	2.29
	Paraonidae sp. 1	2.61	Capitellidae sp. 2	3.73	Hesionidae sp. 4	2.29
	Cirratulidae sp. 6 T+B	1.90	Cirratulidae sp. 1	3.73	Paraonidae sp. 1 A+B	2.29
	Paraonidae sp. 2	1.90	Paraonidae sp. 1	3.73	*Armandia* sp. 1 B	2.29
	Paraonidae sp. 3	1.90	*Brada* sp. 1 T+B	3.11	Paraonidae sp. 12 T+B	2.29

surrounding communities (Levin et al. 2016). For example, mobile benthic predators have been demonstrated to aggregate around seeps (Åström et al. 2018) and include seep-derived carbon in their diets (MacAvoy et al. 2002; MacAvoy et al. 2003), seep productivity may support pelagic bacterial assemblages in the Gulf of Mexico (Kelleyl et al. 1998), and stable isotope analyses suggest that nematode diets include thiotrophic carbon up to 10 m from mud volcano sites in the Gulf of Cádiz (Pape et al. 2011).

The hypothesis that the faunal characteristics of chemotones are driven by energy supplements from active seep habitat gains some further support from our finding that the average carbon stable isotope ($\delta^{13}C$) value of macrofauna collected from chemotone habitat is intermediate between that collected from active and background habitats (Table 2). However, it should be noted that the macrofauna isotopic dataset collected was limited in its replication and skewed toward samples from active seep habitat. That faunal biomass was elevated in chemotones relative to background habitat, but not faunal density, suggests that chemotone individuals have a larger body mass, on average, than individuals in background habitat. It is possible that water column food supplements are utilized predominantly by a subset of the chemotone assemblage that attain large body mass but this food enhancement is not manifested in elevated population densities. Average faunal nitrogen stable isotope ($\delta^{15}N$) values of transition individuals (Table 2), and our analysis of traits, do not provide evidence for a greater density of predatory macrofauna in the chemotone relative to surrounding habitats, although again it should be considered that our

sampling for macrofauna isotopic characterization was limited.

In other environments, such as coastal and riparian zones and caves, food subsidies along gradients from higher productivity habitats to lower have been linked with an increased faunal density and species richness in the ecotone relative to the lower productivity neighboring habitat (Anderson and Polis 1998; Dangerfield et al. 2003; Prouse et al. 2004), although species diversity may not necessarily be elevated in the ecotone (Dangerfield et al. 2003; Prouse et al. 2004). Our results suggest that ecotones associated with chemosynthetic bottom water energy subsidies in the deep sea are associated with a distinct assemblage composition and increased biomass, but similar faunal density and diversity relative to lower-productivity neighboring habitat.

Our finding of a chemotone surrounding methane seeps is consistent with the broader concept of a "sphere of influence" surrounding deep-sea chemosynthetic ecosystems, and suggests that the spatial extent of influence of methane seeps on surrounding environments is greater than might be predicted based on the distributions of seep-associated megafauna alone (Bell et al. 2016; Levin et al. 2016; Demopoulos et al. 2018). Using Mound 12 as an example (the most extensively sampled seep site in this study), we estimate that the chemotone may extend outward for 200 m or more from zones of active seepage (Supplementary Material 1: Fig. S1; Table S1). However, the spatial extent of the chemotone likely varies with seep site depending on seepage characteristics. Future studies should better define the spatial extent and characteristics of seep chemotones by frequent sampling along transects from active seep habitat, through the chemotone, toward background deep-sea habitat.

Conservation of methane seep habitats

Methane seep habitats have been recognized as increasing deep-sea habitat heterogeneity, boosting β diversity, and elevating regional γ diversity (Cordes et al. 2010; Sellanes et al. 2010; Sen et al. 2019). That a distinct chemotone fauna, potentially with habitat endemic species, appears to surround methane seeps reaffirms this perception. Seeps are also associated with the provision of a number of valuable ecosystem services, including carbon sequestration through the production of authigenic carbonates, biogeochemical cycling, habitat provision to commercially important species, and bioprospecting potential (Boetius and Wenzhöfer 2013; Levin et al. 2016; Åström et al. 2020). However, seep habitats are under increasing direct and indirect pressure from current and projected anthropogenic activities including fishing (German et al. 2011; Bowden et al. 2013), oil and gas extraction (German et al. 2011; Cordes et al. 2016), mining, and climate change (Levin and Le Bris 2015; Sweetman et al. 2017). During the *Alvin* dives conducted during cruises AT37-13 and AT42-03, we observed some of the direct pressures on Costa Rican methane seep communities, including lost longline fishing gear and plastic debris. Increasing our understanding of the interaction between deep-sea chemosynthetic communities and surrounding photosynthetically fueled deep-sea communities and how community attributes change along chemotones is essential to the effective management and protection of these systems (Levin et al. 2016).

Our research emphasizes that management and/or conservation efforts in chemosynthetic environments need to be cognisant of the ecological attributes and spatial extent of the chemotone communities surrounding them. Further study of hypothesized chemotones, particularly with regard to microbes, meiofauna, and megafauna, would aid in this endeavor. Moving forward, chemotones should be incorporated into baseline surveys, environmental impact assessments, the design of protected areas, and the valuation of ecosystem services. These considerations have relevance not only to the management of hydrothermal vents and methane seeps, but also to the broad continuum of chemosynthetic ecosystems being discovered.

Data availability statement

All data utilized by this study are freely available through "Figshare" (DOI: 10.6084/m9.figshare.10070282), and as Supplemental Material.

References

Alfaro-Lucas, J. M., and others. 2020. High environmental stress and productivity increase functional diversity along a deep-sea hydrothermal vent gradient. Ecology **101**: e03144.

Anderson, W. B., and G. A. Polis. 1998. Marine subsidies of Island communities in the Gulf of California: Evidence from stable carbon and nitrogen isotopes. Oikos **81**: 75–80.

Ashford, O. S., and others. 2018. Phylogenetic and functional evidence suggests that deep-ocean ecosystems are highly sensitive to environmental change and direct human disturbance. Proc. Roy. Soc. B Biol. Sci. **285**: 20180923.

Åström, E. K. L., M. L. Carroll, W. G. Ambrose Jr., A. Sen, A. Silyakova, and J. L. Carroll. 2018. Methane cold seeps as biological oases in the high-Arctic deep sea. Limnol. Oceanogr. **63**: S209-S231, S1.

Åström, E. K. L., A. Sen, M. L. Carroll, and J. L. Carroll. 2020. Cold seeps in a warming Arctic: Insights for benthic ecology. Front. Mar. Sci. **7**: 244. https://doi.org/10.3389/fmars.2020.00244.

Attrill, M. J., and S. D. Rundle. 2002. Ecotone or ecocline: Ecological boundaries in estuaries. Estuar. Coast. Shelf Sci. **55**: 929–936.

Bell, J. B., and others. 2016. Geochemistry, faunal composition and trophic structure in reducing sediments on the southwest South Georgia margin. R. Soc. Open Sci. **3**: 160284.

Bett, B. J. 2001. UK Atlantic margin environmental survey: Introduction and overview of bathyal benthic ecology. Cont. Shelf Res. **21**: 917–956.

Billett, D. S. M., B. J. Bett, W. D. K. Reid, B. Boorman, and I. G. Priede. 2010. Long-term change in the abyssal NE Atlantic: The "*Amperima* Event" revisited. Deep-Sea Res. II Top. Stud. Oceanogr. **57**: 1406–1417.

Bivand, R., H. Ono, R. Dunlap, and M. Stigler. 2015. Package "classInt", p. Selected commonly used methods for choosing univariate class intervals for mapping or other graphics purposes.

Boetius, A., and F. Wenzhöfer. 2013. Seafloor oxygen consumption fuelled by methane from cold seeps. Nat. Geosci. **6**: 725–734.

Bowden, D. A., A. A. Rowden, A. R. Thurber, A. R. Baco, L. A. Levin, and C. R. Smith. 2013. Cold seep epifaunal communities on the Hikurangi margin, New Zealand: Composition, succession, and vulnerability to human activities. PLoS One **8**: e76869.

Campanyà-Llovet, N., and P. V. R. Snelgrove. 2018. Effects of temporal variation in food sources on infaunal community structure of chemosynthetic and non-chemosynthetic environments in Barkley Hydrates, British Columbia, Canada. Deep Sea Res. I: Oceanogr. Res. Pap. **140**: 118–127.

Carney, R. S. 2005. Zonation of deep biota on continental margins. Oceanogr. Mar. Biol. **43**: 211–278.

Carney, R. S. 2010. Stable isotope trophic patterns in echinoderm megafauna in close proximity to and remote from Gulf of Mexico lower slope hydrocarbon seeps. Deep-Sea Res. II Top. Stud. Oceanogr. **57**: 1965–1971.

Clarke, K. R., and R. N. Gorley. 2006. PRIMER v6: User Manual/Tutorial. PRIMER-E.

Clements, F. E. 1905. Research methods in ecology. Univ. of Nebraska Publishing Company.

Cline, J. D. 1969. Spectrophotometric determination of hydrogen sulfide in natural waters. Limnol. Oceanogr. **14**: 454–458.

Cordes, E. E., and others. 2010. The influence of geological, geochemical, and biogenic habitat heterogeneity on seep biodiversity. Mar. Ecol. **31**: 51–65.

Cordes, E. E., and others. 2016. Environmental impacts of the deep-water oil and gas industry: A review to guide management strategies. Front. Environ. Sci. **4**: 58. https://doi.org/10.3389/fenvs.2016.00058

Cúrdia, J., S. Carvalho, A. Ravara, J. D. Gage, A. M. Rodrigues, and V. Quintino. 2004. Deep macrobenthic communities from Nazaré submarine canyon (NW Portugal). Sci. Mar. **68**: 171–180, S1.

Dangerfield, J. M., and others. 2003. Patterns of invertebrate biodiversity across a natural edge. Austral Ecol. **28**: 227–236.

Demopoulos, A. W. J., J. R. Bourque, A. Durkin, and E. E. Cordes. 2018. The influence of seep habitats on sediment macrofaunal biodiversity and functional traits. Deep-Sea Res. I Oceanogr. Res. Pap. **142**: 77–93.

Demopoulos, A. W. J., D. Gualtieri, and K. Kovacs. 2010. Food-web structure of seep sediment macrobenthos from the Gulf of Mexico. Deep-Sea Res. II Top. Stud. Oceanogr. **57**: 1972–1981.

Flach, E., and W. de Bruin. 1999. Diversity patterns in macrobenthos across a continental slope in the NE Atlantic. J. Sea Res. **42**: 303–323.

Fortin, M.-J., and others. 2000. Issues related to the detection of boundaries. Landsc. Ecol. **15**: 453–466.

Fry, B. 2006. Stable isotope ecology. Springer.

Gage, J. D. 2004. Diversity in deep-sea benthic macrofauna: The importance of local ecology, the larger scale, history and the Antarctic. Deep-Sea Res. II Top. Stud. Oceanogr. **51**: 1689–1708.

Georgieva, M. N., and others. 2020. Evidence of vent-adaptation in sponges living at the periphery of hydrothermal vent environments: Ecological and evolutionary implications. Front. Microbiol. **11**: 1636. https://doi.org/10.3389/fmicb.2020.01636

Gerdes, K. H., and others. 2019. Megabenthic assemblages at the southern Central Indian Ridge – spatial segregation of inactive hydrothermal vents from active-, periphery- and non-vent sites. Mar. Environ. Res. **151**: 104776. https://doi.org/10.1016/j.marenvres.2019.104776.

German, C. R., E. Ramirez-Llodra, M. C. Baker, P. A. Tyler, and ChEss-Scientific-Steering-Committee. 2011. Deep-water chemosynthetic ecosystem research during the census of marine life decade and beyond: A proposed deep-ocean road map. PLoS One **6**: e23259.

Goffredi, S. K., and others. 2020. Methanotrophic bacterial symbionts fuel dense populations of deep-sea feather duster worms (Sabellida, Annelida) and extend the spatial influence of methane seepage. Sci. Adv. **6**: eaay8562.

Gooday, A. J., and others. 2010. Habitat heterogeneity and its influence on benthic biodiversity in oxygen minimum zones. Mar. Ecol. **31**: 125–147.

Gosz, J. R. 1993. Ecotone hierarchies. Ecol. Appl. **3**: 369–376.

Hessler, R. R., and W. M. Smithey. 1983. The distribution and community structure of megafauna at the Galapagos rift hydrothermal vents, p. 735–770.*In* P. A. Rona, K. Boström, L. Laubier, and K. L. Smith [eds.], Hydrothermal processes at seafloor spreading centers. US: Springer.

Jamieson, A. J., and others. 2011. Bait-attending fauna of the Kermadec trench, SW Pacific Ocean: Evidence for an ecotone across the abyssal–hadal transition zone. Deep-Sea Res. I Oceanogr. Res. Pap. **58**: 49–62.

Johnson, N. A., and others. 2007. The relationship between the standing stock of deep-sea macrobenthos and surface production in the western North Atlantic. Deep-Sea Res. I Oceanogr. Res. Pap. **54**: 1350–1360.

Kark, S., and B. J. van Rensburg. 2006. Ecotones: Marginal or central areas of transition? Isr. J. Ecol. Evol. **52**: 29–53.

Kelleyl, C. A., R. B. CofJin, and L. A. Cifuentes. 1998. Stable isotope evidence for alternative bacterial carbon

sources in the Gulf of Mexico. Limnol. Oceanogr. **43**: 1962–1969.

Koulouri, P., C. Dounas, C. Arvanitidis, D. Koutsoubas, and A. Eleftheriou. 2006. Molluscan diversity along a Mediterranean soft bottom sublittoral ecotone. Sci. Mar. **70**: 573–583.

Leduc, D., A. A. Rowden, M. R. Clark, D. A. Bowden, and A. R. Thurber. 2016. Limited differences among habitats in deep-sea macro-infaunal communities off New Zealand: Implications for their vulnerability to anthropogenic disturbance. Mar. Ecol. **37**: 845–866.

Levin, L. A. 2005. Ecology of cold seep sediments: Interactions of fauna with flow, chemistry and microbes. Oceanogr. Mar. Biol. **43**: 1–46.

Levin, L. A., and others. 2016. Hydrothermal vents and methane seeps: Rethinking the sphere of influence. Front. Mar. Sci. **3**: 72.

Levin, L. A., and J. D. Gage. 1998. Relationships between oxygen, organic matter and the diversity of bathyal macrofauna. Deep-Sea Res. II Top. Stud. Oceanogr. **45**: 129–163.

Levin, L. A., C. L. Huggett, and K. F. Wishner. 1991. Control of deep-sea benthic community structure by oxygen and organic-matter gradients in the eastern Pacific Ocean. J. Mar. Res. **49**: 763–800.

Levin, L. A., and N. Le Bris. 2015. The deep ocean under climate change. Science **350**: 766–768.

Levin, L. A., and G. F. Mendoza. 2007. Community structure and nutrition of deep methane-seep macrobenthos from the North Pacific (Aleutian) margin and the Gulf of Mexico (Florida escarpment). Mar. Ecol. **28**: 131–151.

Livingston, B. E. 1903. The distribution of the upland plant societies of Kent County, Michigan. Bot. Gaz. **35**: 36–55.

MacAvoy, S. E., R. S. Carney, C. R. Fisher, and S. A. Macko. 2002. Use of chemosynthetic biomass by large, mobile, benthic predators in the Gulf of Mexico. Mar. Ecol. Prog. Ser. **225**: 65–78.

MacAvoy, S. E., S. A. Macko, and R. S. Carney. 2003. Links between chemosynthetic production and mobile predators on the Louisiana continental slope: Stable carbon isotopes of specific fatty acids. Chem. Geol. **201**: 229–237.

Marcus, J., and V. Tunnicliffe. 2002. Living on the edges of diffuse vents on the Juan de Fuca ridge. Cah. Biol. Mar. **43**: 263–266.

McGinnis, D. F., J. Greinert, Y. Artemov, S. E. Beaubien, and A. Wüest. 2006. Fate of rising methane bubbles in stratified waters: How much methane reaches the atmosphere? J. Geophys. Res. Oceans **111**: C09007. https://doi.org/10.1029/2005JC003183

Menot, L., and others. 2010. Spatial heterogeneity of macrofaunal communities in and near a giant pockmark area in the deep Gulf of Guinea. Mar. Ecol. **31**: 78–93.

Meyer-Dombard, D. A. R., W. Swingley, J. Raymond, J. Havig, E. L. Shock, and R. E. Summons. 2011. Hydrothermal ecotones and streamer biofilm communities in the lower Geyser Basin, Yellowstone National Park. Environ. Microbiol. **13**: 2216–2231.

Nebra, A., C. Alcaraz, N. Caiola, G. Muñoz-Camarillo, and C. Ibáñez. 2016. Benthic macrofaunal dynamics and environmental stress across a salt wedge Mediterranean estuary. Mar. Environ. Res. **117**: 21–31.

Odum, E. P. 1953. Fundamentals of ecology. W. B. Saunders Company.

Oksanen, J. and others. 2013. Vegan: Community ecology package. R package version 2.0-9.

Pape, E., and others. 2011. Community structure and feeding preference of nematodes associated with methane seepage at the Darwin mud volcano (Gulf of Cádiz). Mar. Ecol. Prog. Ser. **438**: 71–83.

Pearson, T. H., and R. Rosenberg. 1978. Macrobenthic succession in relation to organic enrichment and pollution of the marine environment. Oceanogr. Mar Biol. Ann. Rev. **16**: 229–311.

Pohlman, J. W., J. E. Bauer, W. F. Waite, C. L. Osburn, and N. R. Chapman. 2011. Methane hydrate-bearing seeps as a source of aged dissolved organic carbon to the oceans. Nat. Geosci. **4**: 37–41.

Prouse, X., R. L. Ferreira, and R. P. Martins. 2004. Ecotone delimitation: Epigean–hypogean transition in cave ecosystems. Austral Ecol. **29**: 374–382.

R-CoreTeam. 2017. R: A language and environment for statistical computing. R Foundation for Statistical Computing.

Reeburgh, W. S. 1967. An improved interstitial water sampler. Limnol. Oceanogr. **12**: 163–165.

Rex, M. A., and others. 2006. Global bathymetric patterns of standing stock and body size in the deep-sea benthos. Mar. Ecol. Prog. Ser. **317**: 1–8.

Sanders, H. L., R. R. Hessler, and G. R. Hampson. 1965. An introduction to the study of deep-sea benthic faunal assemblages along the Gay Head-Bermuda transect. Deep-Sea Res. Oceanogr. Abstr. **12**: 845–867.

Sellanes, J., C. Neira, E. Quiroga, and N. Teixido. 2010. Diversity patterns along and across the Chilean margin: A continental slope encompassing oxygen gradients and methane seep benthic habitats. Mar. Ecol. **31**: 111–124.

Sen, A., and others. 2019. Image based quantitative comparisons indicate heightened megabenthos diversity and abundance at a site of weak hydrocarbon seepage in the southwestern Barents Sea. PeerJ **7**: e7398.

Sen, A., and others. 2016. Peripheral communities of the Eastern Lau Spreading Center and Valu Fa Ridge: Community composition, temporal change and comparison to near-vent communities. Mar. Ecol. **37**: 599–617.

Smith, C. R., F. C. De Leo, A. F. Bernardino, A. K. Sweetman, and P. M. Arbizu. 2008. Abyssal food limitation, ecosystem structure and climate change. Trends Ecol. Evol. **23**: 518–528.

Sweetman, A. K., and others. 2017. Major impacts of climate change on deep-sea benthic ecosystems. Elementa Sci. Anthrop. **5**. https://doi.org/10.1525/elementa.203

Traut, B. H. 2005. The role of coastal ecotones: A case study of the salt marsh/upland transition zone in California. J. Ecol. **93**: 279–290.

van der Maarel, E. 1990. Ecotones and ecoclines are different. J. Veg. Sci. **1**: 135–138.

Walsh, J. J. 1971. Relative importance of habitat variables in predicting the distribution of phytoplankton at the ecotone of the Antarctic upwelling ecosystem. Ecol. Monogr. **41**: 291–309.

Weston, D. P. 1990. Quantitative examination of macrobenthic community changes along an organic enrichment gradient. Mar. Ecol. Prog. Ser. **61**: 233–244.

Zajac, R. N., R. S. Lewis, L. J. Poppe, D. C. Twichell, J. Vozarik, and M. L. DiGiacomo-Cohen. 2003. Responses of infaunal populations to benthoscape structure and the potential importance of transition zones. Limnol. Oceanogr. **48**: 829–842.

Acknowledgments

We are thankful to the Ministerio de Ambiente y Energía of Costa Rica (Sistema Nacional de Áreas de Conservación/Comisión Nacional para la Gestión de la Biodiversidad) for granting collection permits (AT37-13: SINAC-CUS-PI-R-035-2017, AT42-03: SINAC-SE-064-2018). We are very grateful to the Captains, Crew, Science Party, and *Alvin* team of RV *Atlantis* legs AT37-13 and AT42-03 for facilitating sample collection. We thank Jennifer Le and Odalisca Breedy, Lillian McCormick, Natalya Gallo, and Olivia Pereira for their help with sectioning and preserving push core samples. We thank Jennifer Gonzalez and Olivia Pereira for their help with processing specimens for stable isotope analysis. We thank Sujung Lim for their part in generating the geochemical data analyzed here. We are grateful to three anonymous reviewers, whose insightful and constructive comments helped to strengthen this article. This work was funded by National Science Foundation Ocean Sciences grant numbers 1634172 and 1635219. Author Oliver S. Ashford additionally received support from Scripps Institution of Oceanography as a Postdoctoral Scholar.

Conflict of Interest

None declared.

Submitted 16 May 2020
Revised 17 October 2020
Accepted 18 December 2020

Associate editor: Leila Hamdan